Electronic Supplementary Information

Si Nanoparticle Clusters in Hollow Carbon Capsules (SNC@C) as Lithium Ion Battery Anodes: Toward High Initial Coulombic Efficiency

Tae Jin Kim[1,‡], Jeong Hoon Yoon[2,‡], Gi-Ra Yi[2,*] and Pil J. Yoo[1,*]

[1] SKKU Advanced Institute of Nanotechnology (SAINT), Suwon 16419, Republic of Korea

*E-mail : pjyoo@skku.edu

[2]School of Chemical Engineering, Sungkyunkwan University (SKKU), Suwon 16419, Republic of Korea

*E-mail : yigira@g.skku.edu

S1. Comparative mathematical modeling of the specific surface area between yolk-shell and clustered-core structures.

The mathematical modeling for the specific surface area (SSA) according to the structural variations is comparatively carried out for the yolk-shell and the clustered-core structures. In the case of the yolk-shell structured particles, the thickness of the carbon layer (*t*) is chosen as the variable. Likewise, for clustered-core capsules, the radius (*r*) of the internal cluster is used as the main parameter. The shape of core-shell particles or clustered-core capsules are ideally assumed to be a full sphere with a mono-dispersity in size. In more detail, the yolk-shell structure includes Si core with 40 nm in diameter and 10 nm of interspacing gap with the outer shell. For the case of clustered-core capsules, the same sized Si particles are clustered and encompassed by the outer carbon capsule with a thickness of 10 nm. For a comparison, the total number of internal Si NPs comprising the cluster is set to be identical to that of the yolk-shell structured system.

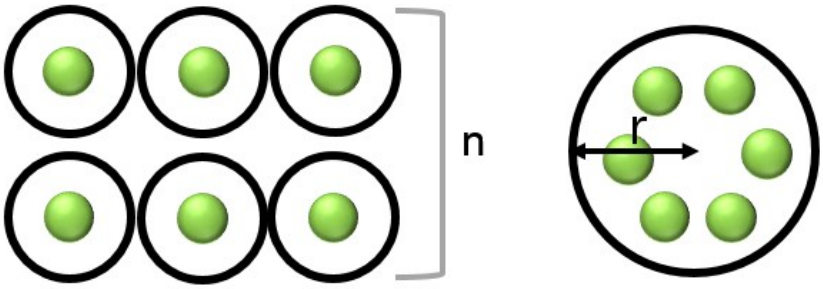

Using above assumptions, we formulate the mass balance equations for Si and carbon, respectively, for yolk-shell particles and clustered-core capsules.

$$\frac{4\pi}{3} * 20^3 * n * \rho_{Si} + \frac{4\pi}{3}\{(30+t)^3 - 30^3\} * n * \rho_c$$

$$= \frac{4\pi}{3} * 20^3 * n * \rho_{Si} + \frac{4\pi}{3}\{r^3 - (r-10)^3\} * \rho_c \quad (1)$$

where ρ_{Si} and ρ_c are the densities of Si and carbon, respectively, and n is the number of Si particles in a single cluster. Since the same weight ratio between Si and carbon is applied for both structures, considered masses for Si and carbon in balance equations need to be equated. Likewise, the relationship between the SSAs for the yolk-shell and clustered-core structures can be derived as follows.

$$\frac{A_{yolk-shell}}{A_{cluster}} = \frac{\{40^2 + (30-t)^2\}n + 20^2 n}{\{r^2 + (r-10)^2\} + 20^2 n} \quad (2)$$

where $A_{\text{yolk-shell}}$ denotes the SSA of the yolk-shell structures and A_{cluster} is the SSA for clustered-core structures. Upon simultaneously solving above two equations, t is subject to the changes of other variables. Therefore, the ratio of SSAs ($A_{\text{yolk-shell}}$ / A_{cluster}) is determined by varied number of n with a specific value of r.

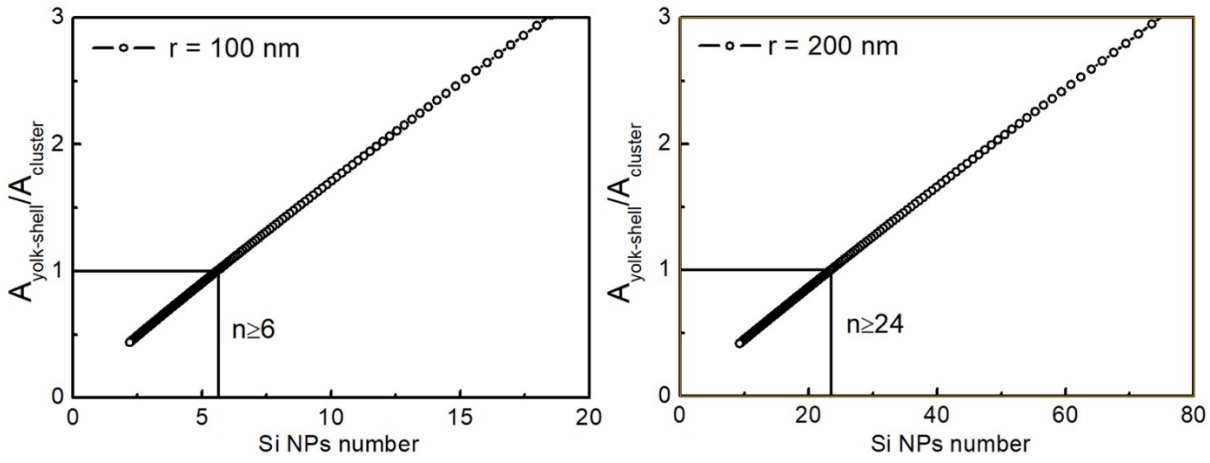

As presented in the Figure, the SSA ratio is mostly linearly varied according to the clustering number of n. For example, for 200 nm-sized clustered core particles (r = 100 nm), the SSA

value of the clustered core capsules is expected to be smaller than that of the yolk-shell structure when n is greater than the critical number of 6.

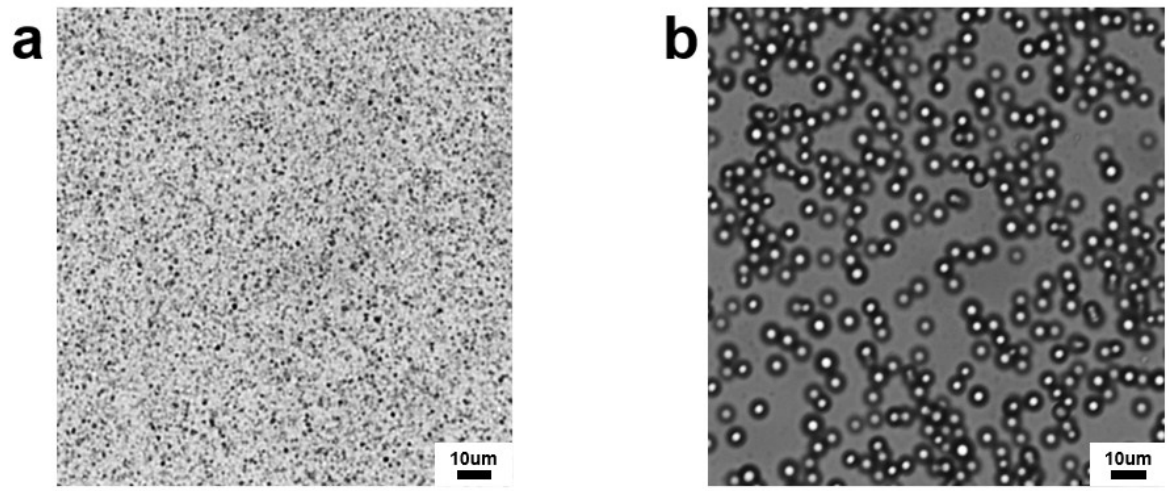

Figure S1. Optical microscopic images of (a) Si-nanoemulsion in SDS solution, (b) St-macroemulsion with 3 μm in size prepared by penetrating through SPG membrane.

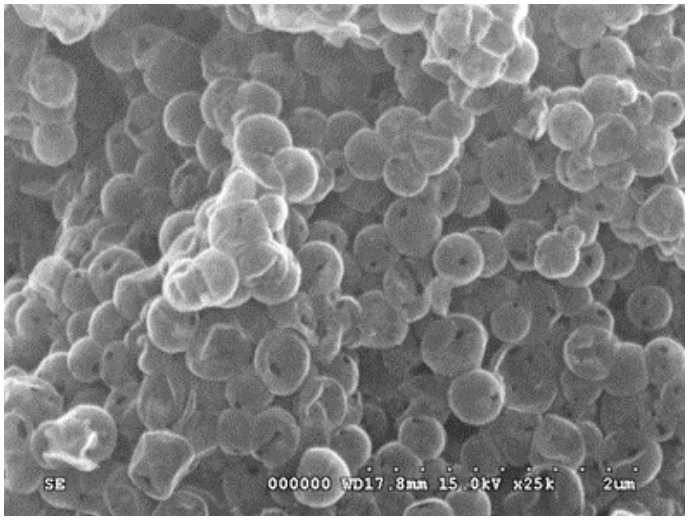

Figure S2. FE-SEM image of SNC@C (m-SC) structure after the pyrolysis.

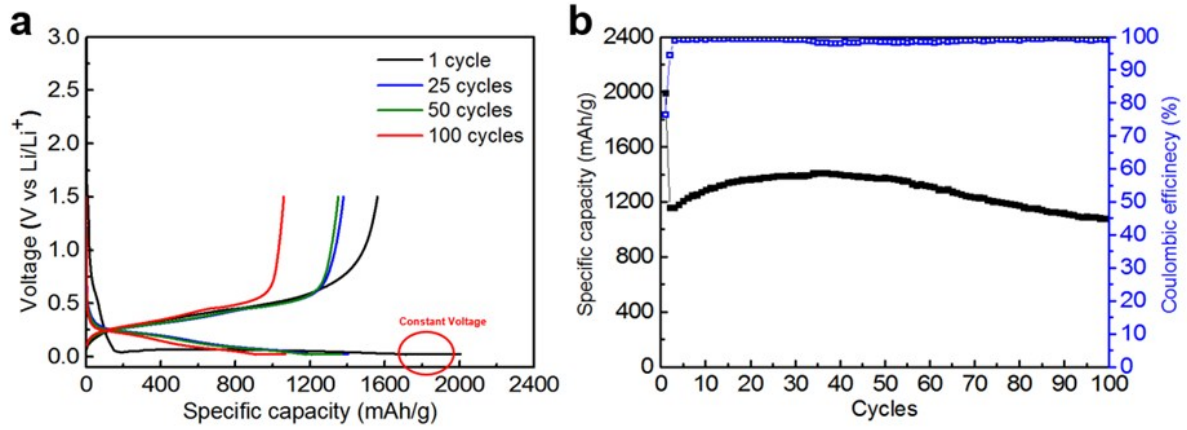

Figure S3. (a) Galvanostatic charge/discharge profiles with constant voltage mode at a 0.02 V cut-off (b) cycling performance of m-SC with constant voltage mode.

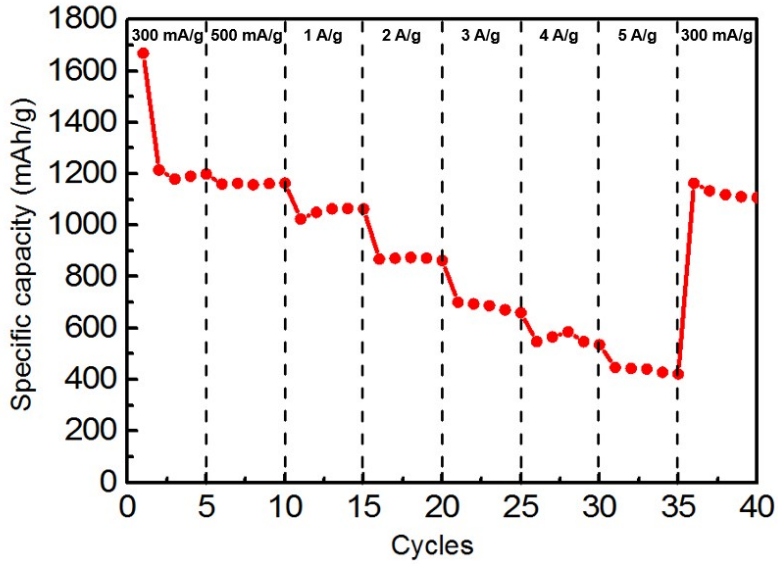

Figure S4. Rate performance of m-SC sample with varying current density ranging from 300

mA/g to 5A/g

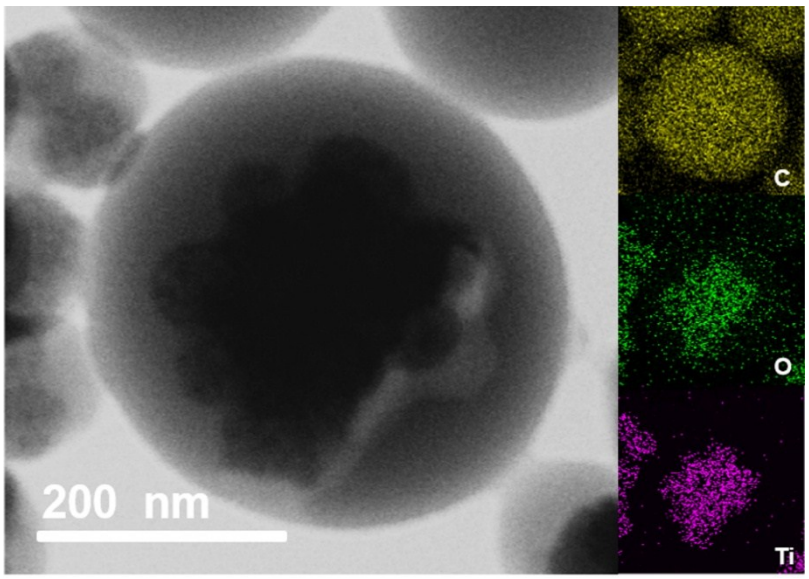

Figure S5. TEM observation of TiO_2-cluster@PS particles and EDS analysis.

Table S1. Synthetic recipes for Si-Nanoemulsion and St-Macroemulsion

	Si-nanoemulsions				Styrene-macroemulsions				
sample	Wt (%)	Octane (ml)	H_2O (g)	SDS (mg)	Styrene (g)	H_2O (g)	SDS (mg)	KPS (mg)	HD (mg)
Latex1	6	4	96	20	5	80	100	20	80
Latex2	3	4	96	20	5	80	100	20	80
Latex3	1	4	96	20	5	80	100	20	80

Table S2. Comparison of the electrochemical performances with other reported Si/C structured anodes.

Si size (nm)	Capacity (mAh/g) (cycle number)	Current density (mA/g)	Initial Coulombic efficiency (%)	Reference
40~70	756 (100)	1^{st} : 100 2^{nd} ~ : 500	81	**This work (h-SC)**
10	1054 (100)	50	80	*Phys.Chem.Chem.Phys.*, 2014, 16, 4135
70	1100 (200)	1^{st} : 100 2^{nd} ~ : 1200	80	*Nano Lett.*. 2017, 17, 1870−1876
80	1160 (1000)	1^{st} : 210 2^{nd}~ : 2100	78	*Nat. Nanotechnol*., 2014, 9, 187–192
40~70	1254 (100)	1^{st} : 100 2^{nd} ~ : 500	77	**This work (m-SC)**
50~100	986 (100)	250	77	*RSC Adv*., 2015, 5, 6782
40~70	987 (100)	1^{st} : 100 2^{nd} ~ : 500	71	**This work (l-SC)**
100	1325 (60)	200	62	*Carbon*, 2018, 127, 424-431
100	1110 (1000)	1^{st} : 400 2^{nd}~10^{th} : 1200 11^{th}~ : 4000	60	*Nano Lett.*, 2012, 12, 3315-3321